Aalborg Universitet

AALBORG UNIVERSITY
DENMARK

Gene expression profiling of subcutaneous adipose tissue reveals new biomarkers in acromegaly

Falch, Camilla M.; Arlien-Søborg, Mai Christiansen; Dal, Jakob; Sundaram, Arvind Y. M.; Michelsen, Annika E.; Ueland, Thor; Olsen, Linn Guro; Heck, Ansgar; Bollerslev, Jens; Jørgensen, Jens Otto L.; Olarescu, Nicoleta C.

Publication date:
2023

Document Version
Publisher's PDF, also known as Version of record

Link to publication from Aalborg University

Gene expression profiling of subcutaneous adipose tissue reveals new biomarkers in acromegaly

Camilla M. Falch,[1,2,3,]* Mai Christiansen Arlien-Søborg,[4,5] Jakob Dal,[6,7]

Arvind Y.M. Sundaram,[8] Annika E. Michelsen,[2,3] Thor Ueland,[2] Linn Guro Olsen,[1] Ansgar Heck,[1,2]

Jens Bollerslev,[1,2] Jens Otto L. Jørgensen,[4] and Nicoleta C. Olarescu[1,2,3]

[1]Section of Specialized Endocrinology, Oslo University Hospital (OUS), Postboks 4950 Nydalen, 0424 Oslo, Norway
[2]Institute of Clinical Medicine, Faculty of Medicine, University of Oslo (UIO), Postboks 1171 Blindern, 0318 Oslo, Norway
[3]Research Institute of Internal Medicine, Oslo University Hospital (OUS), Postboks 4950 Nydalen, 0424 Oslo, Norway
[4]Department of Endocrinology and Internal Medicine, Aarhus University Hospital (AUH), Palle Juul Jensens Boulevard 99, 8200 Aarhus N, Denmark
[5]Medical Research Laboratory, Department of Clinical Medicine, Aarhus University Hospital (AUH), Palle Juul Jensens Boulevard 99, 8200 Aarhus N, Denmark
[6]Department of Endocrinology and Internal Medicine, Aalborg University Hospital (AAUH), Hobrovej 18-22, 9000 Aalborg, Denmark
[7]Steno Diabetes Center North Jutland, Aalborg University Hospital, Søndre Skovvej 3E, 9000 Aalborg, Denmark
[8]Department of Medical Genetics, University of Oslo, Oslo University Hospital, Kirkeveien 166, 0450 Oslo, Norway
*Corresponding author: Section of Specialized Endocrinology, Oslo University Hospital, Postboks 4950 Nydalen, 0424 Oslo, Norway. Email: c.m.falch@studmed.uio.no

Abstract

Context: Active acromegaly is characterized by lipolysis-induced insulin resistance, which suggests adipose tissue (AT) as a primary driver of metabolic aberrations.

Objective: To study the gene expression landscape in AT in patients with acromegaly before and after disease control in order to understand the changes and to identify disease-specific biomarkers.

Methods: RNA sequencing was performed on paired subcutaneous adipose tissue (SAT) biopsies from six patients with acromegaly at time of diagnosis and after curative surgery. Clustering and pathway analyses were performed in order to identify disease activity-dependent genes. In a larger patient cohort ($n = 23$), the corresponding proteins were measured in serum by immunoassay. Correlations between growth hormone (GH), insulin-like growth factor I (IGF-I), visceral AT (VAT), SAT, total AT, and serum proteins were analyzed.

Results: 743 genes were significantly differentially expressed (*P*-adjusted $< .05$) in SAT before and after disease control. The patients clustered according to disease activity. Pathways related to inflammation, cell adhesion and extracellular matrix, GH and insulin signaling, and fatty acid oxidation were differentially expressed.

Serum levels of HTRA1, METRNL, S100A8/A9, and PDGFD significantly increased after disease control ($P < .05$). VAT correlated with HTRA1 ($R = 0.73$) and S100A8/A9 ($R = 0.55$) ($P < .05$ for both).

Conclusion: AT in active acromegaly is associated with a gene expression profile of fibrosis and inflammation, which may corroborate the hypermetabolic state and provide a means for identifying novel biomarkers.

Keywords: growth hormone, IGF-I, RNA sequencing, DXA, disease activity biomarker, cytokines

Significance

The study is the first to investigate by RNA sequencing the gene expression of subcutaneous adipose tissue in paired samples from patients with acromegaly before and after disease control. It demonstrates that active acromegaly increases the expression of genes related to inflammation, extracellular matrix, collagen, and lipid oxidation, supporting and supplying previously published data. The altered appearance and function of adipose tissue drive the disease-specific metabolic aberrations. Additionally, HTRA1, METRNL, S100A8/A9, and PDGFD changed at the protein level in the circulation and correlated to the estimated adipose tissue depots (by dual-energy X-ray absorptiometry [DXA]) and disease activity markers (GH and IGF-I). These proteins' usefulness as novel biomarkers of disease activity and metabolic risk in acromegaly merits future consideration.

Introduction

Acromegaly is a systemic disease caused by a pituitary somatotropinoma, leading to growth hormone (GH) hypersecretion and elevated insulin-like growth factor I (IGF-I) levels.[1] Modern therapy consists of three modalities: surgery, pharmacological treatment, and radiotherapy.[1,2]

Immediate and sustained cure can be achieved by surgery, but the size and configuration of the tumor limit the overall surgical cure rate to approximately 50%.[2-4] GH and IGF-I in serum are used to assess disease control[2], but frequently show discordant results.[5-7] Thus, novel biomarkers of disease activity are needed.

Subcutaneous adipose tissue (SAT) and visceral adipose tissue (VAT) represent the main compartments of adipose tissue (AT) in humans. Increased VAT is associated with insulin resistance and several lifestyle disorders in the general population.[8] However, active acromegaly displays insulin resistance despite a lean rather than obese phenotype.[9,10] This apparent paradox reflects that GH directly stimulates lipolysis and the ensuing elevated levels of free fatty acids induce insulin resistance.[11,12] Recent evidence suggests that GH primarily suppresses insulin-dependent anti-lipolysis in both muscle and fat in healthy human subjects and patients with active acromegaly.[11,13] In addition, inflammatory adipokines may contribute to insulin resistance in acromegaly.[12,14] Recent studies emphasize the association between insulin resistance and SAT due to the mere volume of the latter.[15] Further, inflammation and macrophage infiltration of SAT may facilitate the process.[16] Conversely, there is also evidence that SAT may protect against insulin resistance via capture and subsequent storage of circulating free fatty acids.[17-19]

The aim of the current study was to map gene expression in adipose tissue in patients with acromegaly before and after disease control obtained by pituitary surgery in order to characterize the changes and identify potential biomarkers of disease activity.

Material and methods

Patients and samples

Paired SAT biopsies for RNA sequencing (RNA-seq) were collected from six treatment-naïve patients with acromegaly at diagnosis and after disease control by transsphenoidal surgery only. Patients were followed at Aarhus University Hospital (AUH), Aarhus, Denmark, and were selected based on disease control obtained by surgery alone. These patients participated in a study from which data has previously been published.[13] From Oslo University Hospital (OUS), Oslo, Norway, 17 additional patients were included for further investigation by immunoassay (enzyme-linked immunosorbent assay [ELISA]). Thus, in total, 23 patients were included in the study.

Body composition (including VAT and SAT) was assessed by dual-energy X-ray absorptiometry (DXA, GE Healthcare Lunar Prodigy Advance, Madison, WI, USA). During the study period, different assays for GH and IGF-I were used at OUS, and a random morning GH level (µg/L) was used for the statistical analysis, as described previously.[20] GH levels were measured during an oral glucose tolerance test (OGTT) in both patient groups. IGF-I is presented as the ratio of measured IGF-I values, divided by the age-specific upper limit of normal (IGF-I/ULN). Remission, one year after surgery, was defined as IGF-I/ULN < 1.3, as recommended.[21]

SAT biopsies and RNA extraction

Adipose tissue biopsies were obtained by liposuction from the abdominal subcutaneous fat depots lateral to the umbilicus during local anesthesia, as described.[10] The tissue was immediately washed free of blood, snap-frozen in liquid nitrogen, and stored at −80 °C until use. RNA was extracted from the biopsies using TRIzol (Gibco BRL, Life Technologies, Roskilde, Denmark). RNA was purified using QIAGEN miRNeasy Mini Kit (QIAGEN, Valencia, CA, USA), according to the manufacturer's instructions, including the step for removal of genomic DNA. The amount and purity of total RNA were quantified using a NanoDrop 8000 Spectrophotometer (Thermo Scientific Pierce, Waltham, Maine, USA). RNA integrity was determined by visual inspection of the two ribosomal RNAs on an agarose gel.[10] All RNA integrity numbers (RIN) were above 7, indicating a high RNA quality.[22]

RNA-seq

RNA-seq was performed using 100 ng of RNA for each sample ($n = 12$) at the Norwegian Sequencing Centre, Oslo, Norway. Twelve RNA-seq libraries with unique indexes were prepared using the TruSeq stranded mRNA library prep kit (Illumina, San Diego, CA, USA) by following the manufacturer's instructions. Two batches of six libraries were pooled together, and **150nt** paired-end sequencing was performed on one lane of HiSeq 4000 (Illumina) for each batch. RTA v1.18.66.3 was used for base calling and was further processed using bc2fastq v2.17.1.14 to demultiplex and generate fastq data based on the indexes used during library preparation.

Pre-processing and cleanup

Low-quality reads and adaptors were removed using Trimmomatic v0.33[23] with recommended parameters. BBMap v34.56 (https://sourceforge.net/projects/bbmap) was used to remove reads aligning to PhiX (RefSeq: NC_001422.1), which was added as a spike-in during sequencing.

Transcriptome alignment

Cleaned data were aligned against the Human ensemble GRCh38 (p10, release 90) genome and the transcriptome using Tophat2 v2.0.13,[24] using "–library-type fr-firststrand –no-mixed –no-novel-juncs –transcriptome-index" as parameters. The library size was estimated using the picard v1.112 (https://broadinstitute.github.io/picard/) CollectInsertSizeMetrics tool after aligning the first one million reads using bowtie v2.2.3[25] to human ensemble GRCh38 cDNA sequences, and the output was also provided as parameters for tophat2 alignment. Cuffdiff v2.2.1[26] pipeline was used to calculate the differential expression of the known genes described in ensemble General Feature Format (GTF) and CummeRbund v2.14.[27] R package was used to visualize expression data, and custom scripts were used to create tables and graphs. Hierarchical clustering was performed using Pearson correlation with complete linkage in TM4 MeV (http://mev.tm4.org/).

Heatmap and PCA

A heatmap was generated for transcriptomic data by use of R packages Plotly (https://cran.r-project.org/web/packages/plotly/index.html) and Heatmaply.[28] The heatmap displays significantly expressed transcripts on a *Z*-scored color scale indicating the number of standard deviations that each variable deviates from the variable mean, and the branches are colored according to which second-level branch that they belong to. Principal component analysis (PCA) was performed on complete data without any selection.

Table 1. Patients' characteristics.

A. Aarhus University Hospital (AUH)

	Baseline	After surgery	*P*-value
Age	35.9 (33.8-55.8)	37.2 (35.7-56.7)	—
Sex (women)	3 (50%)	3 (50%)	—
BMI (kg/m^2)	27.5 (24.1-28.9)	24.0 (22.9-29.8)	.463
GH fasting (µg/L)	6.5 (5.0-8.9)	1.5 (1.1-1.8)	.046
GH mean day curve[a] (µg/L)	5.8 (4.0-8.7)	1.4 (1.0-1.5)	.046
IGF-I (µg/L)	551 (335-679)	197 (118-312)	.028
IGF-I/ULN	2.2 (1.3-2.8)	0.8 (0.5-1.2)	.028
Lean body mass (kg)	63.2 (44.4-72.7)	56.9 (44.2-69.0)	.027
Total fat (g)	18 948 (16 717-26 182)	23 706 (17 062-28 213)	.345
Trunk fat (g)	9299 (8097-13 865)	12 260 (8541-15 459)	.345
Glucose (mmol/L)	5.4 (4.7-5.7)	4.7 (4.4-5.0)	.046
HbA1c (mmol/mol)[b]	36 (34-36)	33 (32-35)	.042
HOMA-IR	2.04 (1.1-2.8)	1.1 (0.6-1.3)	.345

B. Oslo University Hospital (OUS)

	Baseline	After surgery	*P*-value
Age	52.7 (45.1-60.0)	54.2 (46.6-61.1)	—
Sex (women)	8 (47%)	8 (47%)	—
BMI (kg/m^2)	31.1 (25.4-32.1)	30.7 (25.6-32.1)	.593
GH random morning (µg/L)	5 (1.7-6.1)	1.6 (0.9-2.7)	.009
GH mean day curve[c] (µg/L)	4.5 (1.8-6.1)	—	—
IGF-I (nmol/L)	98.0 (62.0-119.0)	23.4 (20.0-35.0)	<.001
IGF-I/ULN	2.7 (1.5-3.4)	0.8 (0.7-1.0)	<.001
Lean body mass (kg)	63.3 (49.1-74.6)	63.3 (46.8-68.9)	.001
Total AT (g)	25 107 (23 615-37 731)	30 375 (26 295-40 015)	.017
Trunk fat (g)	14 101 (12 668-18 902)	16 551 (13 905-23 615)	.028
SAT (g)	1576 (1091-2012)	1801 (1354-2487)	.049
VAT (g)	1254 (379-1392)	1217 (542-1827)	.039
Glucose (mmol/L)	6.6 (6.1-7.5)	5.4 (5.1-6.1)	.003
HbA1c (mmol/mol)[d]	41.5 (39-48)	38 (34-43)	.003

Patients' characteristics. A. Describes patients from Aarhus University Hospital (AUH) ($n = 6$). B. Describes Oslo University Hospital (OUS) patients ($n = 17$). Numbers are given in total (%) for categorical measures, and median (IQR) for continuous measures. Baseline values are measured when the acromegaly diagnosis was established, after surgery values are measured when disease control was obtained, and values were analyzed by Wilcoxon matched-pair signed-rank test.

AT, adipose tissue; BMI, body mass index; GH, growth hormone; HOMA-IR, homeostatic model assessment for insulin resistance; IGF-I, insulin-like growth factor I; SAT, subcutaneous adipose tissue; ULN, upper limit of normal; VAT, visceral adipose tissue.

[a]Mean GH levels measured during oral glucose tolerance test (OGTT) for a standardized set of time points before oral glucose was given.
[b]$n = 5$.
[c]$n = 15$.
[d]$n = 14$.

Pathways

All differentially expressed genes (DEGs) (adjusted *P*-value < .05) were included in the pathway analysis (Pathview Web, https://pathview.uncc.edu/).[29] All DEGs were included in an overrepresentation test in Panther-db (http://pantherdb.org/) with Fischer's exact test controlling for false positives by Benjamini Hochberg's false discovery rate (FDR), using Homo sapiens as a reference genome (File S1, Biological process, Cellular component and Molecular function).[30] DEGs with a fold change above 1.9 were considered for network interaction analysis (String database, https://string-db.org), performed with medium confidence while hiding disconnected nodes.[31]

Gene selection

DEGs coding for circulating proteins in blood (as stated on The Human Protein Atlas open source database, https://proteinatlas.org/) with a high fold change (>1.9) in RNA-seq data and/or belonging to significantly differentially expressed pathways were considered ($n = 35$). Of these, after carefully searching the literature (National Library of Medicine [NCBI] gene portal [https://ncbi.nlm.nih.gov/gene/],

UniProt [https://uniprot.org/], The Human Protein Atlas, and PubMed [https://pubmed.ncbi.nlm.nih.gov/]), 11 genes were chosen for further measurement by ELISA in the patient serum samples.

Immunoassay by ELISA

For convenience, the proteins will be referred by their gene nomenclature. The corresponding protein names are listed in File S1, Proteins. The genes S100A8 and S100A9 code for proteins that form a heterodimer S100A8/A9 in vivo; thus, ELISA measurements were performed for the S100A8/A9 complex, and not for the proteins separately. Serum protein levels for ANGPT1, GRN, METRNL, MMP9, PDGFD, PTX3, S100A8/A9, and TEK were measured using commercially available human ELISA DuoSets (R&DSystems, Minnesota, USA). Serum levels of HTRA1 were measured using a precoated ELISA Kit (Cloud-Clone Corp., Texas, USA). Serum levels of FLT1 were measured using a Quantikine ELISA Kit (R&DSystems, Minnesota, USA). All experiments were performed according to the manufacturers' specifications. All samples were applied in duplicate and the washing steps were performed using a BioTek EL406 Combination Washer
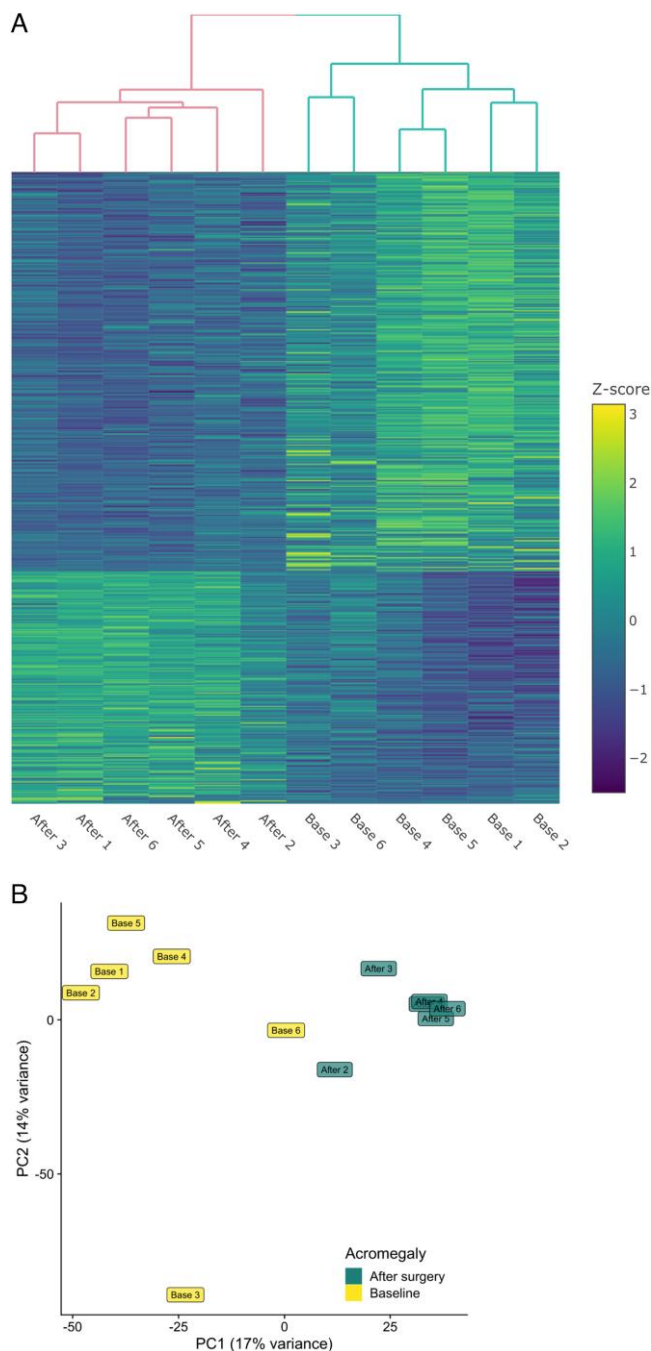
Figure 1. Heatmap of significantly differentially expressed genes and principal component analysis of paired SAT biopsies. (A) Heatmap of RNA sequencing (RNA-seq) differentially expressed genes (DEGs) in Base (active acromegaly) and After (after disease control was obtained by suregery) and (B) principal component analysis (PCA) of complete data without any selection in baseline (active acromegaly) and after surgery (after disease control was obtained by surgery) samples, *n* = 6.

Dispenser (BioTek, Winooski, Vermont, USA). Absorption was read at 450 nm with the wavelength correction set to 540 nm by a Synergy H1 Hybrid Reader (BioTek).

Statistics

Variables were checked for normal distribution by visual methods (histograms and Q–Q plots). Suited transformation methods were performed, where appropriate. Normally distributed data are presented as means (SD) and analyzed by paired *t*-test. Data not normally distributed are presented as median (IQR) and analyzed by Wilcoxon matched-pair signed-rank test. Correlations were analyzed between baseline values and percentwise change in values between baseline and following disease control for serum protein measurements, SAT, VAT, total AT, GH, and IGF-I with non-parametric test (Spearman's rho). Correlation analyses were performed including OUS patients only (*n* = 17), because SAT and VAT values were not measured in AUH patients. For this reason, patient data are presented separately for OUS and AUH patients, given in total (%) for categorical measures and median (IQR) for continuous measures, and analyzed by Wilcoxon matched-pair signed-rank test. The statistical analyses were performed using SPSS version 26 and STATA version 16.1. Two-sided *P*-values < .05 were considered significant.

Ethics

Written informed consent was obtained from all patients. The study was approved by the regional ethics committee (Central Denmark Region Scientific Ethics Committee (M-20070130), registered at ClinicalTrials.gov (NCT00647179), and conducted in agreement with the Declaration of Helsinki II and Regional committees for medical and healthcare research ethics (Oslo, REK no.: 15240) and hospital authority. The genetic expression analyses were exclusively related to SAT biology. Thus, no information about the patient's genotype was given, and the study did not influence treatment or patient follow-up.

Results

Clinical characteristics of patients

Clinical characteristics of patients are presented in Table 1 for AUH patients (A), and OUS patients (B). There was an equal sex distribution in both patient populations, and median (IQR) age at diagnosis was 36 (34-56) years for AUH patients, and 53 (45-60) years for OUS patients. The median time from the baseline visit to the post-operative visit was 0.7 (0.6-2.0) and 1.3 (1.2-1.5) years for AUH and OUS patients, respectively. Following surgery, there was a significant decrease in GH, IGF-I, glucose, HbA1c, and lean body mass measurements in both groups (Table 1, AUH patients: *P* < .05 for all; OUS patients: *P* < .01 for all), whereas only a significant increase of the fat depots (Total AT, Trunk fat, SAT, and VAT) was observed in OUS patients (*P* < .05 for all). In both groups, there was no significant change in the body mass index (BMI).

RNA-seq

RNA-seq resulted in 34-81 million 150 PE reads across the 12 samples where the depth was above the recommended value reviewed by Liu et al. (2014).[32] Bioinformatics analyses revealed 743 DEGs: 470 genes upregulated and 273 downregulated at baseline compared to after disease control (*P*-adjusted < .05) (File S1, DEGs). As shown in Figure 1, heatmap analysis with hierarchical clustering and principal component analysis (PCA) showed that samples grouped according to disease activity without exception.

Pathways

Pathways significantly differentially expressed between baseline and after disease control are presented as a complete list in File S1, Pathways. Signaling pathways of interest for the

Table 2. Pathways significantly differentially expressed between baseline and after disease control.

Signaling pathway	Genes	
	Upregulated	Downregulated
Inflammation		
hsa04650 natural killer cell-mediated cytotoxicity	CD247, TYROBP, HLA-A, HRAS, RAC2, VAV1, FCGR3B, ITGB2	PIK3CA
hsa04668 TNF signaling pathway	MAPK11, MAPK13, ATF4, CREB3L1, CEBPB, FOS, SOCS3, MMP9, MMP14, VCAM1, AKT1	CREB1, PIK3CA, ITCH
hsa04660 T cell receptor signaling pathway	AKT1, HRAS, FOS, VAV1, CD247, MAPK11, MAPK13	PIK3CA, DLG1
hsa04062 chemokine signaling pathway	CXCR4, VAV1, AKT1, HRAS, RAC2, PIK3R5	JAK2, PIK3CA, GNG2, ROCK1, ROCK2
hsa04670 leukocyte transendothelial migration	MMP9, ITGB2, MAPK11, MAPK13, CYBA, NCF4, VAV1, RAC2, CXCR4, VCAM1	AFDN, ITGB1, PIK3CA, ROCK1, ROCK2, ARHGAP5
hsa04066 HIF-1 signaling pathway	IGF1, AKT1, PFKL, HMOX1, EIF4EBP1	EGFR, PIK3CA, FLT1, ANGPT1, TEK, BCL2
hsa04145 phagosome	FCGR3B, ITGB2, CYBA, NCF4, TUBB2A, TUBB4B, SEC61B, HLA-DOA, HLA-DRA, HLA-A, HLA-F	ITGAV, ITGB1, PIKFYVE, HLA-DRB5
hsa04060 cytokine–cytokine receptor interaction	LTB, IL3RA, CSF2RA, CXCR4, TNFRSF12A	BMP3, BMP6, LIFR, GHR
Cell adhesion, collagen, and ECM		
hsa04810 regulation of actin cytoskeleton	PFN1, RAC2, VAV1, FGD3, ITGB2, HRAS, RRAS, PDGFD, CXCR4	SCIN, PIKFYVE, PPP1R12B, ROCK1, ROCK2, PIK3CA, ITGAV, ITGB1, EGFR, FGF2
hsa04514 cell adhesion molecules (CAMs)	ITGB2, VCAM1, HLA-DOA,HLA-DRA, HLA-A, HLA-F, CD276	ITGB1, NFASC, ITGAV, HLA-DRB5
hsa04510 focal adhesion	AKT1, ZYX, COL1A1, COL1A2, COL6A1, COL6A2, COL6A6, CCND1, HRAS, IGF1, PDGFD, RAC2, VAV1	ITGB1, ITGAV, PPP1R12B, ROCK1, ROCK2, PIK3CA, ARHGAP5, BCL2, EGFR, FLT1, MET
GH and insulin signaling		
hsa04630 Jak-STAT signaling pathway	AKT1, SOCS3, CSF2RA, IL3RA, CCND1, HRAS	PIK3CA, BCL2, STAM2, JAK2, EGFR, GHR, LIFR
hsa04151 PI3K-Akt signaling pathway	EIF4EBP1, AKT1, CCND1, IGF1, PDGFD, HRAS, DDIT4, PIK3R5, COL1A1, COL1A2, COL6A1, COL6A2, COL6A6, IL3RA, ATF4, CREB3L1	PIK3CA, EGFR, ERBB4, FLT1, MET, TEK, ANGPT1, FGF2, GNG2, ITGAV, ITGB1, GHR, JAK2, CREB1, BCL2

Signaling pathways significantly differentially expressed between baseline and after disease control. Differentially expressed genes (DEGs) upregulated in baseline or downregulated in baseline (ie, upregulated after disease control) are listed for the applicable pathway.

study question and DEGs involved in these pathways are listed in Table 2. These pathways were related to inflammation, cell adhesion and extracellular matrix (ECM), and GH and insulin signaling. Figure 2 shows an interaction network analysis between DEGs with a fold change > 1.9. Three large clusters were identified: one containing genes related to inflammation, the second containing genes related to collagen and ECM, and the third containing genes involved in fatty acid beta-oxidation. Gene Ontology (GO) biological process analysis (File S1, Biological process) identified collagen and ECM as being overexpressed in active acromegaly, whereas glucose and lipid metabolism and insulin signaling regulation were predominantly present following disease control. GO analysis showed increased cellular components and molecular functions in mitochondria, collagen, and ECM in active disease (File S1, Cellular component and Molecular function).

Gene selection

Of the 743 significant DEGs, 315 genes presented a fold change > 1.9, and 96 belonged to the significantly differentially expressed pathways. Of these, 35 coded for proteins secreted to the circulation (Table 3). We selected 11 of these genes for immunoassay (Table 3A) based on their previously described roles. HTRA1, METRNL, S100A8, S100A9, PDGFD, PTX3, GRN, and MMP9 were upregulated in baseline samples, and FLT1, ANGPT1, and TEK were upregulated after disease control.

ELISA

Figure 3 presents the increase in serum protein measurements between baseline and following disease control for HTRA1 (mean [SD] 74.4 [31.6] vs. 96.3 [51.3] ng/mL, $P \leq .001$), METRNL (median [IQR] 1.7 [1.1-1.9] vs. 1.8 [1.5-2.0] ng/mL, $P = .001$), S100A8/A9 (mean [SD] 601 [422] vs. 922 [551] ng/mL, $P = .005$), and PDGFD (mean [SD] 1.5 [0.5] vs. 1.6 [0.4] ng/mL, $P = .031$). For all these proteins, serum levels increased between baseline and after disease control, whereas the gene expression in SAT decreased for the corresponding genes (File S1, RNAseq_ELISA). One explanation could be that the circulating levels of these proteins only to a limited degree stem from SAT. Alternatively, the increase in total SAT mass after treatment may overall translate into increased protein production. It is also possible that ECM matrix remodeling after disease control may impact on the production of proteins in SAT.

The difference in PDGFD remained significant also when adjusted for the patients' platelet count ($P = .003$). There was no significant difference between baseline and after samples for MMP9 ($P = .506$), GRN ($P = .394$), PTX3 ($P = .094$), TEK ($P = .536$), ANGPT1 ($P = .584$), and FLT1 ($P = .175$). The difference in MMP9 remained unchanged after adjusting for platelet count ($P = .177$).

Correlations

Correlation analyses of the baseline serum protein levels showed a negative correlation between METRNL and GH ($R = -0.59$, $P = .015$) and S100A8/A9 and GH ($R = -0.56$,
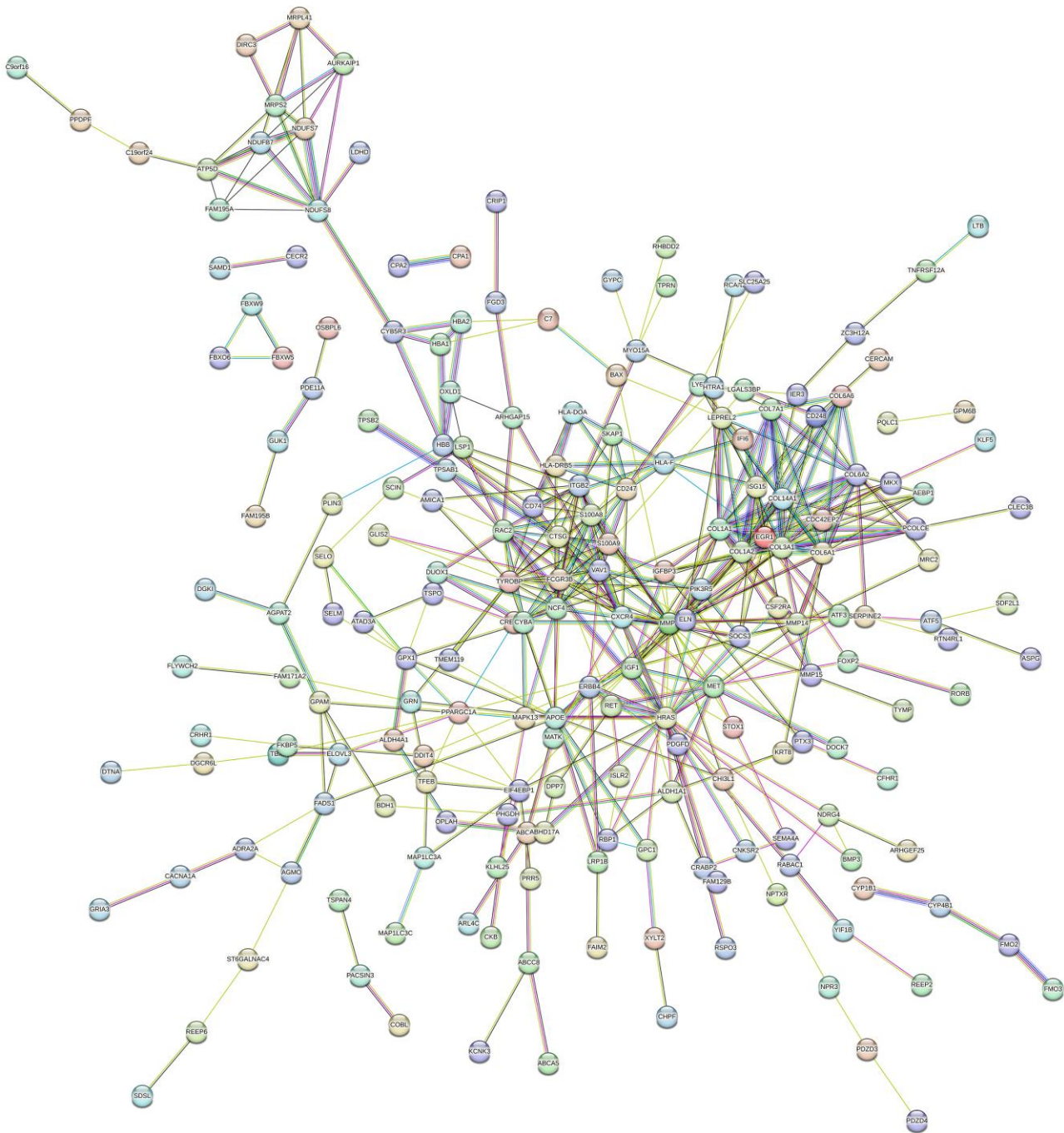
Figure 2. Interaction network analysis of differentially expressed genes. Interaction network analysis presenting differentially expressed genes (DEGs) (fold change > 1.9) between baseline and after disease control interactions. Performed with medium confidence while hiding disconnected nodes. For the interactive, online figure, see hyperlink in File S1, Interaction network.

P = .021) and positive correlations between S100A8/A9 and VAT and total AT (R = 0.74, P = .001, and R = 0.61, P = .010, respectively) (Figure 4). Correlations of the variables expressed as percentage change showed a positive correlation between HTRA1 and VAT (R = 0.55, P = .024) and between S100A8/A9 and VAT (R = 0.72, P = .001) and a negative correlation between PFGFD and GH (R = −0.64, P = .007).

Discussion

In this study, we demonstrate that acromegaly disease activity impacts on the mRNA signature of SAT and overplays the

inter-individual differences, suggesting a strong and consistent effect. Further, collagen and ECM, inflammation, and mitochondria β-oxidation pathways decrease significantly in SAT following disease control. Novel candidate genes upregulated in SAT in active acromegaly include HTRA1, METRNL, S100A8/A9, and PDGFD, which may represent potential biomarkers for disease activity and metabolic risk factors in these patients.

A higher number of upregulated genes were present in active disease as compared to remission, supporting experimental studies in bovine growth hormone transgenic (bGH) mice where pathways related to fatty acid oxidation, branched-chain

Table 3. Significantly differentially expressed genes coding for proteins secreted in the circulation.

A. Selected genes

Gene	Gene description	Fold change	*P*-adjusted	Involvement in significant signaling pathway
PTX3	Pentraxin 3	18.60	.006	
S100A8	S100 calcium binding protein A8	5.12	.003	
S100A9	S100 calcium binding protein A9	4.36	.003	
PDGFD	Platelet-derived growth factor D	3.13	.003	
MMP9	Matrix metallopeptidase 9	2.80	.003	TNF signaling pathway. Leukocyte transendothelial migration. Estrogen signaling pathway
METRNL	Meteorin-like, glial cell differentiation regulator	2.32	.003	
HTRA1	HtrA serine peptidase 1	2.00	.003	
GRN	Granulin precursor	1.93	.003	Regulation of actin cytoskeleton. HIF-1 signaling pathway. Endocytosis. PI3K-Akt signaling pathway. Estrogen signaling pathway. MAPK signaling pathway
ANGPT1	Angiopoietin 1	1.75	.003	HIF-1 signaling pathway. PI3K-Akt signaling pathway. MAPK signaling pathway
TEK	TEK receptor tyrosine kinase	1.65	.003	HIF-1 signaling pathway. PI3K-Akt signaling
FLT1	fms-related tyrosine kinase 1	1.46	.039	HIF-1 signaling pathway

B. Not selected genes

Gene	Gene description	Fold change	*P*-adjusted	Involvement in significant signaling pathway
CFHR1	Complement factor H-related 1	6.11	.006	
FCGR3B	Fc fragment of IgG receptor IIIb	3.65	.015	Osteoclast differentiation. Natural killer cell-mediated cytotoxicity. Phagosome
APOL4	Apolipoprotein L4	3.59	.003	
TPSAB1	Tryptase alpha/beta 1	3.15	.003	
IGFBP3	Insulin-like growth factor-binding protein 3	3.07	.003	
ISG15	ISG15 ubiquitin-like modifier	2.96	.003	
CHI3L1	Chitinase 3-like 1	2.74	.008	
PTGDS	Prostaglandin D2 synthase	2.73	.003	
TPSB2	Tryptase beta 2 (gene/pseudogene)	2.46	.015	
C7	Complement C7	2.36	.010	
IGF1	Insulin-like growth factor I	2.31	.015	
CLEC3B	C-type lectin domain family 3 member B	2.26	.003	
C1QTNF6	C1q and TNF-related 6	2.17	.027	
APOE	Apolipoprotein E	2.17	.003	
LGALS3BP	Galectin 3-binding protein	2.09	.003	
MET	tRNA aspartic acid methyltransferase 1	2.08	.003	Axon guidance
EMC10	ER membrane protein complex subunit 10	2.05	.003	
C1QTNF5	C1q and TNF-related 5	2.05	.003	
CSF2RA	Colony-stimulating factor 2 receptor alpha subunit	2.01	.048	Jak-STAT signaling pathway. Cytokine–cytokine receptor interaction
XYLT2	Xylosyltransferase 2	2.01	.003	
NUCB1	Nucleobindin-1	1.96	.003	
BMP6	Bone morphogenetic protein 6	1.87	.015	Cytokine–cytokine receptor interaction
GHR	Growth hormone receptor	1.71	.006	Cytokine–cytokine receptor interaction
EGFR	Epidermal growth factor receptor	1.43	.047	Focal adhesion

Table describes the 35 genes coding for proteins secreted in blood and includes genes selected (A) and not selected (B) for immunoassay. Selection was based on fold change more than 1.9 or involvement in significantly differentially expressed signaling pathway and previously described roles.

amino acid degeneration, and the immune system were upregulated in SAT.[33] Additionally, a RNA-seq study comparing the AT from patients with active acromegaly and patients with non-functioning pituitary adenomas as controls found a higher number of DEGs in patients with acromegaly.[34] Similarly to our results, genes involved in fatty acid metabolism were upregulated in AT in the active acromegaly group, whereas genes involved in inflammation were downregulated. However, the absence of prospective data comparing active and controlled acromegaly is a limitation.[34]

Our data showed that collagen and ECM genes were consistently upregulated in active acromegaly, which is compatible with studies in mouse models,[35-37] and support the hypothesis that increased fibrosis in SAT impairs its ability to store free fatty acids and thereby contributes to systemic insulin resistance. The remaining question to be answered is which cell type in the AT (eg, mature adipocyte, fibroblast, and stromal vascular fraction) is the driver of fibrosis.

Many mitochondria genes were upregulated in active disease, which support the observations that GH modulates mitochondria function in liver and adipose tissues.[38,39]

Based on the results of this study, it could be speculated that treatment decreasing the GH systemic load and SAT signaling, as well as anti-fibrotic and insulin-sensitizing medications, might alleviate some of the metabolic disturbances and symptoms in acromegaly.
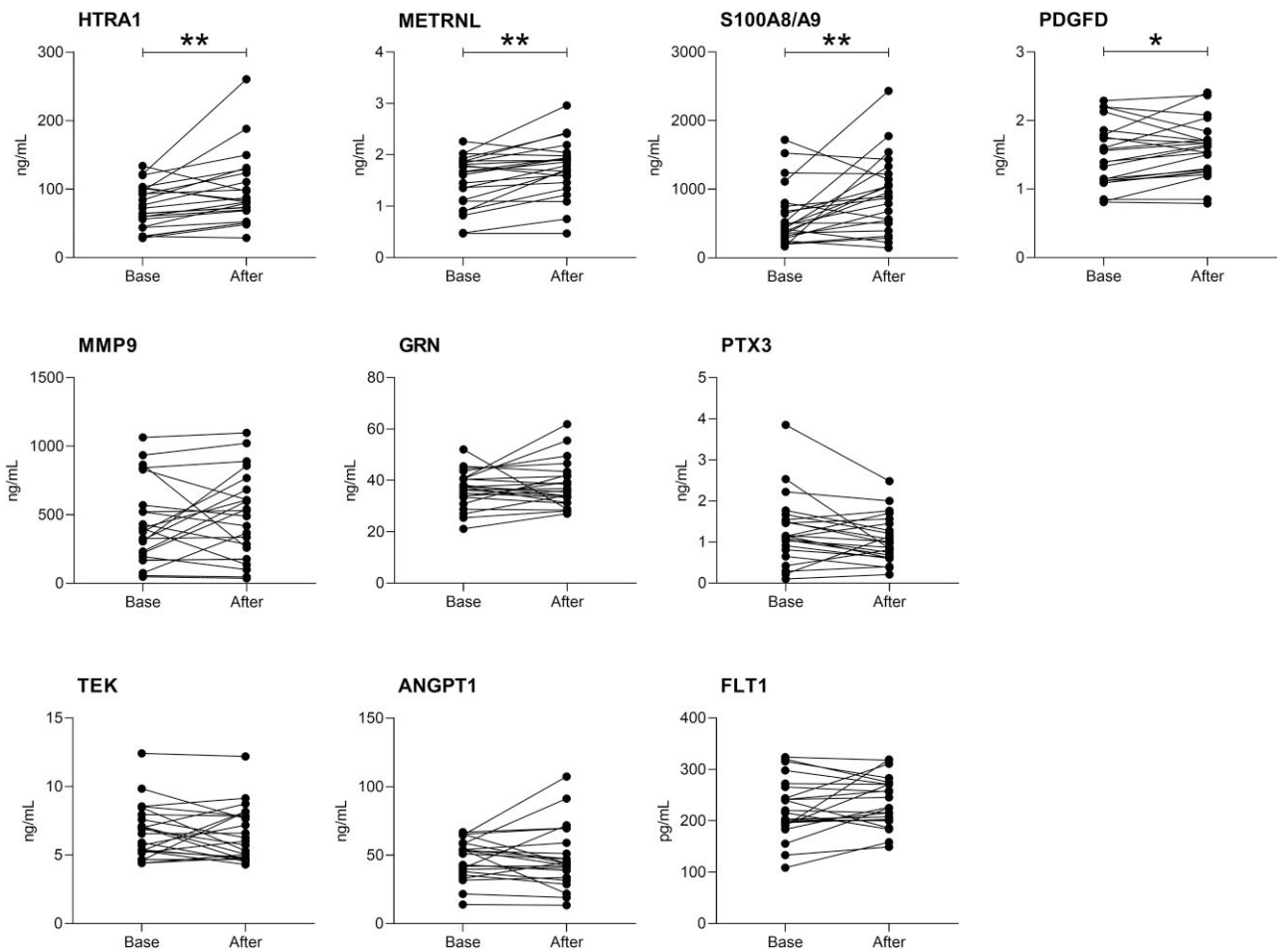
Figure 3. Protein levels in serum at baseline and after surgery. Serum protein levels of HTRA1, METRNL, S100A8/A9, PDGFD, MMP9, GRN, PTX3, TEK, ANGPT1 (ng/mL), and FLT1 (pg/mL). Significant change between Base (baseline samples) and After (after disease control samples) is marked *$P < .05$ and **$P < .01$ ($n = 23$).

A causal link between GH-induced lipolysis and insulin resistance is well-established.[11] In healthy human subjects, acute GH exposure downregulates the G0/G1 switch gene (G0S2) and fat specific protein 27 (FSP27), both of which are important suppressors of lipolysis.[13] In addition, phosphatase and tensin homolog (PTEN), which suppresses insulin signaling, was upregulated by GH in SAT.[13] In vitro data has suggested that GH acts via MEK to suppress G0S2.[13] Accordingly, HRAS, an upstream MEK activator, was increased in SAT in active disease in our study. Moreover, active acromegaly impairs insulin signaling in both adipose tissue and muscle.[10] Conversely, our study showed that G0S2 was significantly upregulated in SAT of active acromegaly, whereas no difference was recorded for FSP27 and PTEN. An explanation may be that G0S2 is differently regulated with acute vs. chronic GH exposure.

Our data contributes to the notion of an anti-insulin effect of GH by identifying SORBS1, a protein required for insulin-stimulated glucose transport,[40] and PIK3CA, involved in insulin signaling,[41] to be downregulated in active disease.

TCF/LEF, the read out of canonical Wnt-signaling activation, was increased in active disease supporting the hypothesis on the impairment of mesenchymal stem cell (MSC) differentiation toward adipocytes.[14] Moreover, PPARG coactivator 1 alpha (PPARGC1A), a transcriptional coactivator that regulates genes involved in energy metabolism and mitochondria

biogenesis, and a marker of brown/beige adipocytes[42] was decreased, and Perilipin 3 (PLIN3), a protein required for the formation and maintenance of lipid storage droplets[43] and an inhibitor of beige adipocytes and thermogenic gene expression[44] was increased, suggesting perhaps a decreased beigeing of SAT in active disease. In addition, ADRA2A, known to reduce lipolysis,[45] was increased in active disease, perhaps as an adaptive mechanism.

Growth hormone receptor (GHR) and JAK2 (ie, GHR principal mediator) genes were decreased at baseline and increased significantly following treatment. This could represent adaptation to increased circulating GH levels present in active acromegaly. SOCS3 and SOCS4 (not known to be GHR dependent) were increased in active disease, in addition to IGF-I, IGFBP3, IGFBP4, and IGFBP5, suggesting that AT is able to produce the corresponding proteins in active disease.

Surprisingly, we recorded reciprocal disease activity changes in SAT gene expression of HTRA1, METRNL, S100A8/A9, and PDGFD versus the corresponding protein levels in serum. Gene expression decreased after disease control, whereas the opposite was true for the circulating protein levels. One explanation could be that the circulating levels of these proteins only to a limited degree stem from SAT. Alternatively, the increase in total SAT mass after treatment may overall translate into increased protein production. It is also possible that ECM matrix remodeling after disease
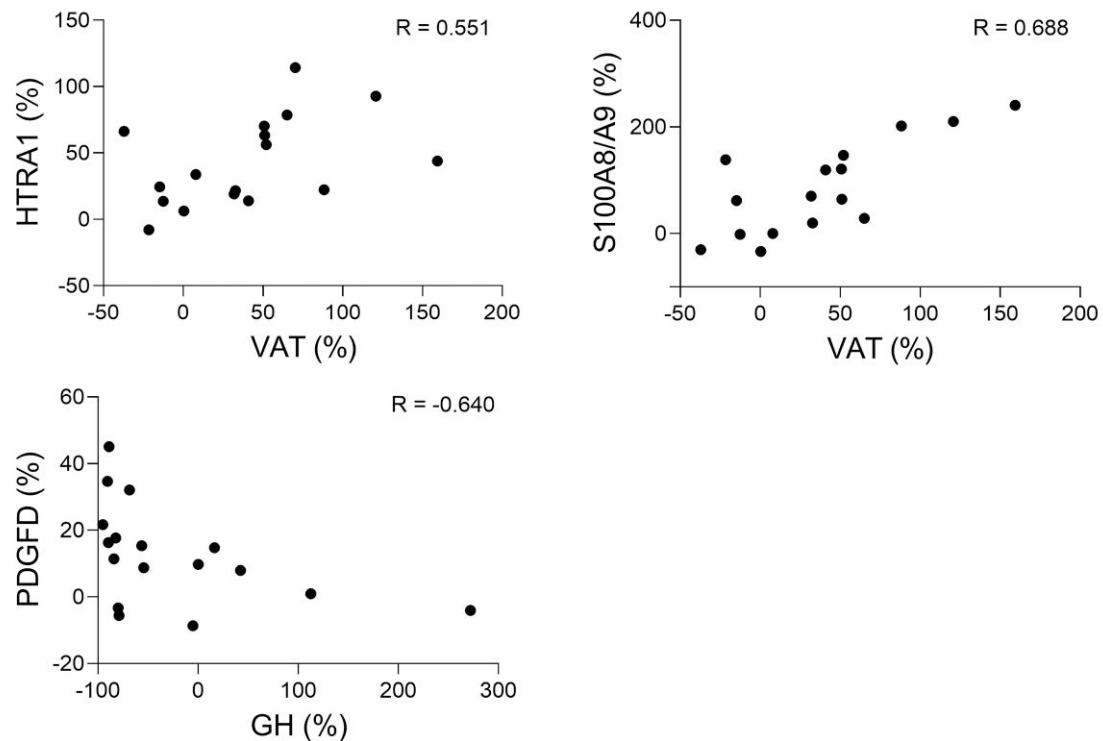
Baseline values
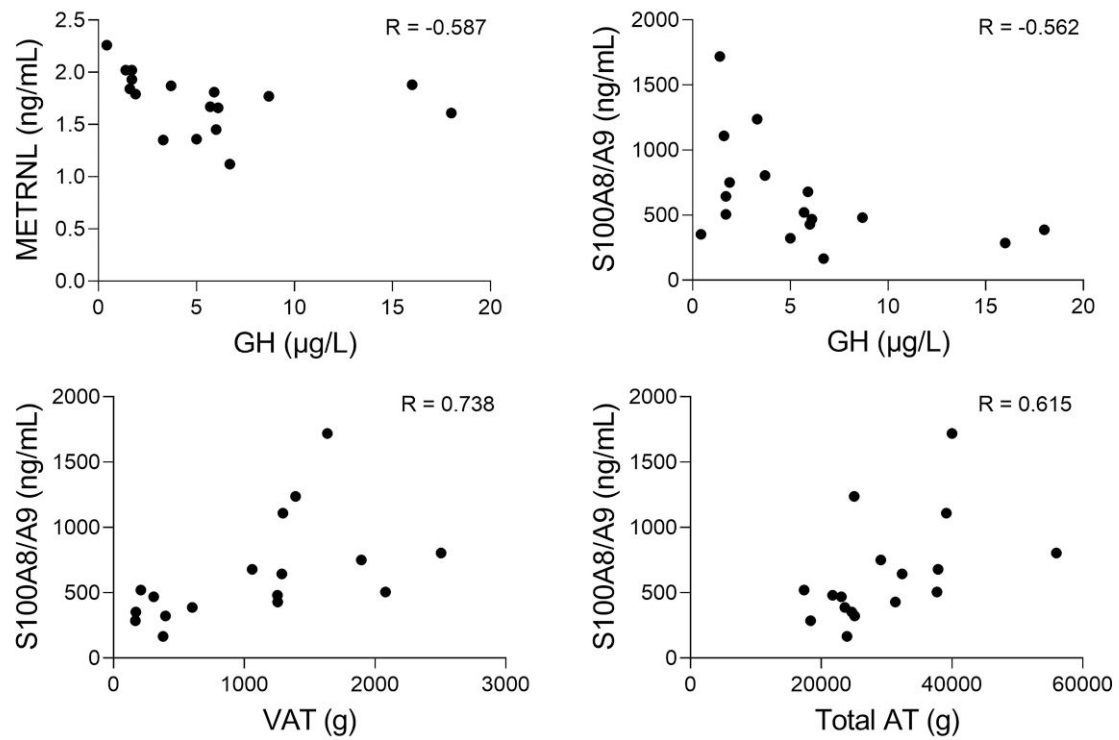
Percent of change values

Figure 4. Correlations. Correlation plots describing significant correlations between serum protein levels (HTRA1, METRNL, S100A8/A9, and PDGFD, ng/mL) and GH, VAT, and total AT (g) ($P < .05$). Correlations analyzed for baseline measurements, and percent of change between baseline and after disease remission (%) measurements ($n = 17$). One outlier was excluded in the analysis between S100A8/A9 (%) and VAT (%).

control may impact on the production of proteins in SAT.[46] The lack of coherence between circulating levels and SAT gene expression may suggest that this approach is not best suited to identify circulating protein targets, and perhaps, blood proteomic profiling could have more merit.

HTRA1 is a serine protease presumed to be involved in the regulation of IGF availability by cleaving the IGF binding proteins.[47] In active acromegaly, we did not find any correlation between the serum levels of HTRA1 and GH or IGF-I levels. However, we found that the increase of serum HTRA1 protein levels correlated to the increase in VAT. HTRA1 might play a role in ECM.[48] In addition to HTRA1, different gene expression of MMPs (MMP9, MMP14, MMP15, ADAM22, and MMP24OS) were upregulated in active disease in our study, suggesting an active collagen/ECM remodeling process. The upregulated gene expression of HTRA1, IGF-I, and IGFBP5 seems to be disease specific since they were recently described to be downregulated in an insulin-resistant obese adolescent population.[49]

METRNL, which was upregulated in active disease, has been identified as a novel adipokine secreted by adipose tissue and skeletal muscle.[50,51] METRNL induces the expression of genes associated with browning of fat, thermogenesis, and adipocyte differentiation and has an anti-inflammatory role. It also stimulates energy expenditure and improves glucose tolerance, but conflicting data prevail as regards the circulating METRNL levels in obesity and T2DM.[50,51] Serum METRNL was negatively correlated to GH levels, contrary to the RNA-seq data.

In active acromegaly, serum S100A8/S100A9 correlated negatively to GH levels, suggesting a limited low-grade inflammation process. As described, S100A8/A9 is mainly secreted by neutrophils and macrophages, and GH has been shown to decrease both S100A8 and S100A9 in human peripheral blood leukocytes.[52] In addition, our results show that S100A8/S100A9 closely reflects VAT mass and total AT mass in active disease and also the increase of VAT with treatment. The strong negative and positive correlation between this protein and GH and AT mass, respectively, could suggest enhanced leukocyte infiltration in adipose tissue in active acromegaly. This is consistent with reports of adipose tissue inflammation in these patients,[12] which could contribute to systemic insulin resistance. The decrease in both S100A8 and S100A9 in adipose tissue, and increased circulating S100A8/A9 levels following surgery, could thus potentially reflect enhanced leukocyte trafficking after disease control.

Considering its role in AT, PDGFD was previously described as a growth factor, promoting inflammation, angiogenesis, and fibrosis[53,54] likely contributing to the changes observed in active acromegaly.

The limitations of the study

As a whole tissue RNA-seq study, it does not provide single-cell resolution data. However, it is the first study to investigate disease activity-dependent changes in SAT. The number of patients included in the ELISA cohort is rather small, allowing for type 2 error. Nevertheless, the cohorts have the advantages of close follow-up and reliable clinical and biochemical variables.

Conclusion

Active acromegaly increases the expression of genes related to inflammation, collagen and ECM, and lipid oxidation. Of the

investigated DEGs, HTRA1, METRNL, S100A8/A9, and PDGFD also changed at the serum protein level. The usefulness of these proteins as novel biomarkers of acromegaly merits future scrutiny.

References

1. Melmed S, Bronstein MD, Chanson P, *et al.* A consensus statement on acromegaly therapeutic outcomes. *Nat Rev Endocrinol.* 2018;14(9):552-561. https://doi.org/10.1038/s41574-018-0058-5
2. Katznelson L, Laws ER Jr, Melmed S, *et al.* Acromegaly: an endocrine society clinical practice guideline. *The J Clin Endocrinol Metab.* 2014;99(11):3933-3951. https://doi.org/10.1210/jc.2014-2700
3. Bollerslev J, Fougner SL, Berg JP. New directions in pharmacological treatment of acromegaly. *Expert Opin Invest Drugs.* 2009;18(1):13-22. https://doi.org/10.1517/13543780802554357
4. Starnoni D, Daniel RT, Marino L, Pitteloud N, Levivier M, Messerer M. Surgical treatment of acromegaly according to the 2010 remission criteria: systematic review and meta-analysis. *Acta Neurochir (Wien).* 2016;158(11):2109-2121. https://doi.org/10.1007/s00701-016-2903-4
5. Freda PU. Monitoring of acromegaly: what should be performed when GH and IGF-1 levels are discrepant? *Clin Endocrinol.* 2009;71(2):166-170. https://doi.org/10.1111/j.1365-2265.2009.03556.x
6. Rubeck KZ, Madsen M, Andreasen CM, Fisker S, Frystyk J, Jorgensen JO. Conventional and novel biomarkers of treatment outcome in patients with acromegaly: discordant results after somatostatin analog treatment compared with surgery. *Eur J*

Endocrinol. 2010;163(5):717-726. https://doi.org/10.1530/EJE-10-0640

7. Schilbach K, Gar C, Lechner A, *et al.* Determinants of the growth hormone nadir during oral glucose tolerance test in adults. *Eur J Endocrinol.* 2019;181(1):55-67. https://doi.org/10.1530/EJE-19-0139

8. Tchernof A, Després JP. Pathophysiology of human visceral obesity: an update. *Physiol Rev.* 2013;93(1):359-404. https://doi.org/10.1152/physrev.00033.2011

9. Olarescu NC, Ueland T, Lekva T, *et al.* Adipocytes as a source of increased circulating levels of nicotinamide phosphoribosyltransferase/visfatin in active acromegaly. *J Clin Endocrinol Metab.* 2012;97(4):1355-1362. https://doi.org/10.1210/jc.2011-2417

10. Arlien-Søborg MC, Dal J, Madsen MA, *et al.* Reversible insulin resistance in muscle and fat unrelated to the metabolic syndrome in patients with acromegaly. *EBioMedicine.* 2022;75:103763. https://doi.org/10.1016/j.ebiom.2021.103763

11. Hjelholt AJ, Charidemou E, Griffin JL, *et al.* Insulin resistance induced by growth hormone is linked to lipolysis and associated with suppressed pyruvate dehydrogenase activity in skeletal muscle: a 2×2 factorial, randomised, crossover study in human individuals. *Diabetologia.* 2020;63(12):2641-2653. https://doi.org/10.1007/s00125-020-05262-w

12. Olarescu NC, Bollerslev J. The impact of adipose tissue on insulin resistance in acromegaly. *Trends Endocrinol Metab.* 2016;27(4):226-237. https://doi.org/10.1016/j.tem.2016.02.005

13. Hjelholt AJ, Lee KY, Arlien-Søborg MC, *et al.* Temporal patterns of lipolytic regulators in adipose tissue after acute growth hormone exposure in human subjects: a randomized controlled crossover trial. *Mol Metab.* 2019;29:65-75. https://doi.org/10.1016/j.molmet.2019.08.013

14. Olarescu NC, Berryman DE, Householder LA, *et al.* GH action influences adipogenesis of mouse adipose tissue-derived mesenchymal stem cells. *J Endocrinol.* 2015;226(1):13-23. https://doi.org/10.1530/JOE-15-0012

15. Patel P, Abate N. Role of subcutaneous adipose tissue in the pathogenesis of insulin resistance. *J Obes.* 2013;2013:489187. https://doi.org/10.1155/2013/489187

16. Apovian CM, Bigornia S, Mott M, *et al.* Adipose macrophage infiltration is associated with insulin resistance and vascular endothelial dysfunction in obese subjects. *Arterioscler Thromb Vasc Biol.* 2008;28(9):1654-1659. https://doi.org/10.1161/ATVBAHA.108.170316

17. Rosen ED, Spiegelman BM. What we talk about when we talk about fat. *Cell.* 2014;156(1-2):20-44. https://doi.org/10.1016/j.cell.2013.12.012

18. Hocking S, Samocha-Bonet D, Milner K-L, Greenfield JR, Chisholm DJ. Adiposity and insulin resistance in humans: the role of the different tissue and cellular lipid depots. *Endocr Rev.* 2013;34(4):463-500. https://doi.org/10.1210/er.2012-1041

19. Tchkonia T, Thomou T, Zhu Y, *et al.* Mechanisms and metabolic implications of regional differences among fat depots. *Cell Metab.* 2013;17(5):644-656. https://doi.org/10.1016/j.cmet.2013.03.008

20. Olarescu NC, Heck A, Godang K, Ueland T, Bollerslev J. The metabolic risk in patients newly diagnosed with acromegaly is related to fat distribution and circulating adipokines and improves after treatment. *Neuroendocrinology.* 2016;103(3-4):197-206. https://doi.org/10.1159/000371818

21. Giustina A, Barkhoudarian G, Beckers A, *et al.* Multidisciplinary management of acromegaly: a consensus. *Rev Endocr Metab Disord.* 2020;21(4):667-678. https://doi.org/10.1007/s11154-020-09588-z

22. Fleige S, Pfaffl MW. RNA Integrity and the effect on the real-time qRT-PCR performance. *Mol Aspects Med.* 2006;27(2-3):126-139. https://doi.org/10.1016/j.mam.2005.12.003

23. Bolger AM, Lohse M, Usadel B. Trimmomatic: a flexible trimmer for illumina sequence data. *Bioinformatics.* 2014;30(15):2114-2120. https://doi.org/10.1093/bioinformatics/btu170

24. Kim D, Pertea G, Trapnell C, Pimentel H, Kelley R, Salzberg SL. Tophat2: accurate alignment of transcriptomes in the presence of insertions, deletions and gene fusions. *Genome Biol.* 2013;14(4):R36. https://doi.org/10.1186/gb-2013-14-4-r36

25. Langmead B, Salzberg SL. Fast gapped-read alignment with Bowtie 2. *Nat Methods.* 2012;9(4):357-359. https://doi.org/10.1038/nmeth.1923

26. Trapnell C, Roberts A, Goff L, *et al.* Differential gene and transcript expression analysis of RNA-seq experiments with TopHat and Cufflinks. *Nat Protoc.* 2012;7(3):562-578. https://doi.org/10.1038/nprot.2012.016

27. Goff L, Trapnell C, Kelley D. cummeRbund: Analysis, exploration, manipulation, and visualization of Cufflinks high-throughput sequencing data. 2022. https://www.bioconductor.org/packages/devel/bioc/manuals/cummeRbund/man/cummeRbund.pdf

28. Galili T, O'Callaghan A, Sidi J, Sievert C. Heatmaply: an R package for creating interactive cluster heatmaps for online publishing. *Bioinformatics.* 2018;34(9):1600-1602. https://doi.org/10.1093/bioinformatics/btx657

29. Luo W, Pant G, Bhavnasi YK, Blanchard SG Jr, Brouwer C. Pathview Web: user friendly pathway visualization and data integration. *Nucleic Acids Res.* 2017;45(W1):W501-W508. https://doi.org/10.1093/nar/gkx372

30. Thomas PD, Campbell MJ, Kejariwal A, *et al.* PANTHER: a library of protein families and subfamilies indexed by function. *Genome Res.* 2003;13(9):2129-2141. https://doi.org/10.1101/gr.772403

31. Szklarczyk D, Gable AL, Lyon D, *et al.* STRING V11: protein-protein association networks with increased coverage, supporting functional discovery in genome-wide experimental datasets. *Nucleic Acids Res.* 2019;47(D1):D607-D613. https://doi.org/10.1093/nar/gky1131

32. Liu Y, Zhou J, White KP. RNA-seq differential expression studies: more sequence or more replication? *Bioinformatics.* 2014;30(3):301-304. https://doi.org/10.1093/bioinformatics/btt688

33. Duran-Ortiz S, Young JA, Jara A, *et al.* Differential gene signature in adipose tissue depots of growth hormone transgenic mice. *J Neuroendocrinol.* 2020;32(11):e12893. https://doi.org/10.1111/jne.12893

34. Hochberg I, Tran QT, Barkan AL, Saltiel AR, Chandler WF, Bridges D. Gene expression signature in adipose tissue of acromegaly patients. *PLoS One.* 2015;10(6):e0129359. https://doi.org/10.1371/journal.pone.0129359

35. Householder LA, Comisford R, Duran-Ortiz S, *et al.* Increased fibrosis: a novel means by which GH influences white adipose tissue function. *Growth Horm IGF Res.* 2018;39:45-53. https://doi.org/10.1016/j.ghir.2017.12.010

36. Kopchick JJ, Basu R, Berryman DE, Jorgensen JOL, Johannsson G, Puri V. Covert actions of growth hormone: fibrosis, cardiovascular diseases and cancer. *Nat Rev Endocrinol.* 2022;18(9):558-573. https://doi.org/10.1038/s41574-022-00702-6

37. List EO, Berryman DE, Buchman M, *et al.* GH knockout mice have increased subcutaneous adipose tissue with decreased fibrosis and enhanced insulin sensitivity. *Endocrinology.* 2019;160(7):1743-1756. https://doi.org/10.1210/en.2019-00167

38. Yang M, Hu B, Sun D, *et al.* Growth hormone receptor gene influences mitochondrial function and chicken lipid metabolism by AMPK-PGC1α-PPAR signaling pathway. *BMC Genomics.* 2022;23(1):219. https://doi.org/10.1186/s12864-021-08268-9

39. Fellinger P, Wolf P, Pfleger L, *et al.* Increased ATP synthesis might counteract hepatic lipid accumulation in acromegaly. *JCI Insight.* 2020;5(5):e134638. https://doi.org/10.1172/jci.insight.134638

40. Lesniewski LA, Hosch SE, Neels JG, *et al.* Bone marrow-specific Cap gene deletion protects against high-fat diet-induced insulin resistance. *Nat Med.* 2007;13(4):455-462. https://doi.org/10.1038/nm1550

41. Hopkins BD, Goncalves MD, Cantley LC. Insulin-PI3K signalling: an evolutionarily insulated metabolic driver of cancer. *Nat Rev Endocrinol.* 2020;16(5):276-283. https://doi.org/10.1038/s41574-020-0329-9

42. Harms M, Seale P. Brown and beige fat: development, function and therapeutic potential. *Nat Med*. 2013;19(10):1252-1263. https://doi.org/10.1038/nm.3361

43. Liu R, Lee J-H, Li J, *et al.* Choline kinase alpha 2 acts as a protein kinase to promote lipolysis of lipid droplets. *Mol Cell*. 2021;81-(13):2722-2735.e9. https://doi.org/10.1016/j.molcel.2021.05.005

44. Lee YK, Sohn JH, Han JS, *et al.* Perilipin 3 deficiency stimulates thermogenic beige adipocytes through PPARα activation. *Diabetes*. 2018;67(5):791-804. https://doi.org/10.2337/db17-0983

45. Garg A, Sankella S, Xing C, Agarwal AK. Whole-exome sequencing identifies ADRA2A mutation in atypical familial partial lipodystrophy. *JCI Insight*. 2016;1(9):e86870. https://doi.org/10.1172/jci.insight.86870

46. Blache U, Stevens MM, Gentleman E. Harnessing the secreted extracellular matrix to engineer tissues. *Nat Biomed Eng*. 2020;4(4):357-363. https://doi.org/10.1038/s41551-019-0500-6

47. Zumbrunn J, Trueb B. Primary structure of a putative serine protease specific for IGF-binding proteins. *FEBS Lett*. 1996;398(2-3):187-192. https://doi.org/10.1016/S0014-5793(96)01229-X

48. Tiaden AN, Richards PJ. The emerging roles of HTRA1 in musculoskeletal disease. *Am J Pathol*. 2013;182(5):1482-1488. https://doi.org/10.1016/j.ajpath.2013.02.003

49. Minchenko DO, Tsymbal DO, Davydov VV, Minchenko OH. Expression of genes encoding IGF1, IGF2, and IGFBPs in blood of obese adolescents with insulin resistance. *Endocr Regul*. 2019;53(1):34-45. https://doi.org/10.2478/enr-2019-0005

50. Alizadeh H. Meteorin-like protein (Metrnl): a metabolic syndrome biomarker and an exercise mediator. *Cytokine*. 2022;157:155952. https://doi.org/10.1016/j.cyto.2022.155952

51. Cheng J-X, Yu K. New discovered adipokines associated with the pathogenesis of obesity and type 2 diabetes. *Diabetes Metab Syndr Obes*. 2022;15:2381-2389. https://doi.org/10.2147/DMSO.S376163

52. Chung L, Nelson AE, Ho KK, Baxter RC. Proteomic profiling of growth hormone-responsive proteins in human peripheral blood leukocytes. *J Clin Endocrinol Metab*. 2009;94(8):3038-3043. https://doi.org/10.1210/jc.2009-0778

53. Folestad E, Kunath A, Wågsäter D. PDGF-C and PDGF-D signaling in vascular diseases and animal models. *Mol Aspects Med*. 2018;62:1-11. https://doi.org/10.1016/j.mam.2018.01.005

54. Zhang Z-B, Ruan C-C, Lin J-R, *et al.* Perivascular adipose tissue-derived PDGF-D contributes to aortic aneurysm formation during obesity. *Diabetes*. 2018;67(8):1549-1560. https://doi.org/10.2337/db18-0098